Application Note

Cell Analysis

Agilent

Trusted Answers

Continuous, Label-Free Monitoring of Immune Cell Clustering and Proliferation Using Agilent xCELLigence RTCA eSight

Authors

Tian Wang, Grace Yang, and Peifang Ye
Agilent Biosciences Co. Ltd.
Hangzhou, China

Ryan Raver, Alejandra Felix, Nancy Li, and Yama Abassi
Agilent Technologies, Inc.
San Diego, CA, USA

Abstract

A hallmark of immunotherapy is the reliance on the cytotoxic effects of T and natural killer (NK) cells on tumor lesions. Immune cell cluster formation is an important sign of T cell activation, as well as an indication of the normal natural killing ability of NK cells. Clustering and proliferation can significantly affect immune cell cytotoxic activity, requiring an easy way to monitor these characteristics and evaluate killing efficacy. Using brightfield to track activated immune cells, the Agilent xCELLigence RTCA eSight automatically recognizes clustering, enabling real-time monitoring and quantitative analysis of immune cell activation and proliferation.

Here, we evaluate CAR-T and NK92 cell activation and clustering using an image-based readout, and target-cell killing efficacy by an impedance-based readout. Our results show that immune cell proliferation capacity and killing efficacies are highly correlated, highlighting the utility of the xCELLigence RTCA eSight. The platform provides an efficient way to dynamically monitor immune cell activation, clustering, and proliferation to advance tumor immunotherapy development.

Introduction

When active, both T and NK cells play a critical role in the immune system, clearing infected cells and pathogens to eliminate disease. Immune response is stimulated via T cell exposure to, and recognition of, antigens—presented by major histocompatibility complex (MHC) molecules—on antigen-presenting cells. Activated T cells aggregate into clusters and proliferate—an action that plays a regulatory role in T cell differentiation and killing efficacy.[1,2] Similarly, healthy and active NK cells also proliferate in a clustered manner. NK cells can be activated through several mechanisms that promote cell clustering, proliferation, and immune cell killing.[3] It is not entirely clear how cell clusters regulate killing efficacy, underscoring a need to monitor the formation and size of cell aggregation, as well as determine the relation to immune cell activation, proliferation, and killing efficacy.

Now, various immune cell surface proteins have been identified as feasible markers to monitor immune cell behavior. Imaging is typically used to detect surface markers related to cytotoxic activation, such as CD8+ on T cells, to visualize infiltration and aggregation at tumor sites.[4] Combining targeted fluorescent labeling and traditional microscopy has become a classical method to observe immune cell behavior, as it has been shown to be direct and accurate. It is unclear, however, if labeling reagents exhibit any interference on immune cell activity, as dynamic changes in cell-cell interactions regulate cytotoxicity and the extent of immune response.

This application note presents a real-time visual and quantitative analysis of immune cell activation and proliferation without additional labels using the xCELLigence RTCA eSight. In vitro activation and proliferation of T and NK-92 cells were monitored by xCELLigence RTCA eSight's imaging capability, while the impedance detection method was used to evaluate the killing potency of CAR-T cells on tumor cells.

Assay principle

To date, the xCELLigence RTCA eSight is currently the only instrument that integrates both microscopic live cell imaging with real-time impedance detection in the same well. The instrument has five cradles; three cradles require specialized plates to collect both impedance and imaging, while the other two are suitable for common cell culture plates, and only collect imaging data. Cellular impedance is continuously measured by gold biosensors integrated at the bottom of Agilent electronic plate (E-Plate) VIEW microplates to evaluate cell number, proliferation rate, cell size and shape, and the strength of cell-matrix adhesion. The impedance signal is recorded at a user-defined time frequency (every minute, hour, etc.) and reported using a unitless parameter called the Cell Index. Changes in target cells (cell shrinkage, detachment, death, lysis, etc.) associated with immune cell killing are easily detected as a drop in Cell Index (impedance). Note that impedance provides a sensitive readout of immobilized target cells; nonadherent immune cells do not contribute to impedance.

At the center of each E-Plate VIEW well, a microscopic window allows xCELLigence RTCA eSight to capture brightfield and fluorescent (red, green, and blue) images from the same cell population. Using a proprietary algorithm, xCELLigence RTCA eSight software can recognize immune cell clusters based on brightness and contrast characteristics captured by brightfield images without requiring fluorescent labeling. Additionally, immune cell cluster recognition is not affected by inclusion of target cells growing in monolayers in immune cell killing assays. As such, xCELLigence RTCA eSight software can rapidly quantify immune cell activation and proliferation by cluster area and count.

Experimental

Materials and methods

Cell maintenance and assays were conducted at 37 °C/5% CO_2. Cell lines or primary cells and their growth media are shown in Table 1. Fetal bovine serum (FBS) was from Gibco (part number 10099-141) and pen/strep was from HyClone (part number SV30010).

Table 1. Cells and media used for the assays.

Cell Lines/ Primary Cells	Base Medium	Medium Supplements
PBMCs, CAR-T cells, Raji	RPMI (Gibco, p/n 11875-093)	10% FBS + 1% pen/strep
K562	IMEM (Gibco, p/n A10489-01)	10% FBS + 1% pen/strep
NK-92	MEM α, no nucleosides (Gibco, p/n 12561-056)	0.2 mM inositol + 0.1 mM 2-mercaptoethanol + 0.02 mM folic acid + 100 to 200 U/mL recombinant IL-2 + 12.5% horse serum + 12.5% fetal bovine serum
A549	Ham's F-12 (Gibco, p/n 11765-054)	10% FBS + 1% pen/strep

T cell activation

First, 96-well plates (Corning, part number 3599) were coated with 5 µg/mL anti-CD3 (T&L Biotechnology, part number GMP-TL101) for 3 hours at room temperature and washed twice with D-PBS to remove excess antibodies. Then, PBMCs were isolated from LeukoPak (Ori Biotech, part number PB007) by Ficoll (Cytiva, part number 17144002)

density gradient centrifugation. Freshly isolated PBMCs were suspended in complete RPMI-1640 medium, and PBMCs (in 200 µL media) were seeded into anti-CD3-precoated 96-well plates at the density of 10, 20, 30, 40, and 50 thousand cells per well. The cell suspension was supplemented with 2 µg/mL anti-CD28 (T&L Biotechnology, part number GMP-TL102) and 10 ng/mL IL-2 (T&L Biotechnology, part number GMP-TL104). In parallel, PBMCs were seeded into uncoated wells as a control. The plate was left at room temperature for 30 minutes, loaded onto xCELLigence RTCA eSight, and images were captured every 2 hours for 5 days.

T cell labeling

A 0.63 µL amount of CD45-BV421 antibody (BioLegend, part number 368521) was added into 200 µL culture medium after T cells were activated, and then proliferated for nine days. Fluorescent images were captured by xCELLigence RTCA eSight after 16 hours of antibody incubation.

Anti-CD19 CAR-T killing of Raji

Raji and K562 green cells, which express a nuclear-localized green fluorescent protein, were produced by transducing parental cells with Agilent eLenti Green reagent (part number 8711010). Then, 72 hours after transduction, the growth medium was changed to one containing 2 µg/mL puromycin for an additional 14 days to select for transductants.

Cryopreserved anti-CD19 CAR-T cells were thawed and prelabeled with 10x Agilent eLive Red reagent (part number 8711004) for 30 minutes. Cells were washed to remove excess dye. Specifics about CAR gene construction and the subsequent cell manufacturing protocol cannot be disclosed at this time as the project was completed in collaboration with another company.

Agilent E-Plate VIEW microplates (part number 300601030) were coated with 4 µg/mL anti-CD40 tethering reagent from the Agilent IMT Assay (anti-CD40) Tethering kit (part number 8100005) or anti-CD71 tethering reagent from the Agilent IMT Assay (anti-CD71) Tethering kit (part number 8100017) at room temperature for 3 hours. The wells were then washed twice with D-PBS to remove excessive antibodies. After measuring the background impedance with 50 µL/well of the medium, 20,000 Raji or K562 cells (100 µL/well) were seeded to each well. Nonadherent target cells were immobilized at the bottom of the E-Plate with anti-CD40 and anti-CD71 coating respectively. After the target cells proliferated overnight, varying numbers of anti-CD19 CAR-T cells (in 50 µL media) were added to achieve a series of effector target ratios (2.5:1, 1.25:1, 0.62:1, 0.31:1, 0.16:1, 0.078:1, 0.39:1, 0.02:1, or 0.01:1).

Impedance was measured every 15 minutes and images were acquired every 120 minutes. In each well, four fields of view (images) were captured in each channel (brightfield, red fluorescence, and green fluorescence). The exposure times were as follows: red (200 ms), green (200 ms), and brightfield (automatically optimized by xCELLigence RTCA eSight).

NK-92 killing of A549

A549 red cells were produced by transducing parental cells with Agilent eLenti Red reagent (part number 8711011). Then, 72 hours after transduction, the growth medium was changed to contain 2 µg/mL puromycin for an additional 14 days to select for transductants.

An assay to determine NK-92 killing of A549 cells was also conducted on E-Plate VIEW microplates as described previously. After adding 50 µL of media per well, the background impedance was measured. Then, 8,000 A549 red cells in 100 µL complete media were seeded into each well. After allowing cells to settle for 30 minutes at room temperature, the E-Plate was loaded into the impedance and imaging cradles (1, 2, or 3). While impedance was measured every 15 minutes, images (four fields of view per well) were collected every 2 hours using the 10x objective. While brightfield settings were automatically adjusted by the instrument, exposures in red were manually set to 300 ms. After monitoring cell adhesion and proliferation overnight, the E-Plate was removed, and 50 µL media containing varying counts of NK-92 was added to achieve a series of E:T ratios (6:1, 3:1, 1.5:1, 0.75:1, 0.38:1, 0.19:1). NK-92 cell activation and cytotoxicity were then continuously monitored, and real-time cellular analysis was performed.

Results and discussion

In vitro T cell activation and clustering

To dynamically observe T cell activation and proliferation *in vitro*, PBMCs were seeded and placed in the xCELLigence RTCA eSight to capture images in real time. As shown in Figure 1A, clusters formed 72 hours after cells were treated with anti-CD3/anti-CD28/IL-2 (seeding density: 50,000 cells/well), although they were not observed in the absence of costimulation. Clusters were recognized by xCELLigence RTCA eSight software based on brightfield images captured (cyan mask) and shown to be highly correlated with manual cluster identification.

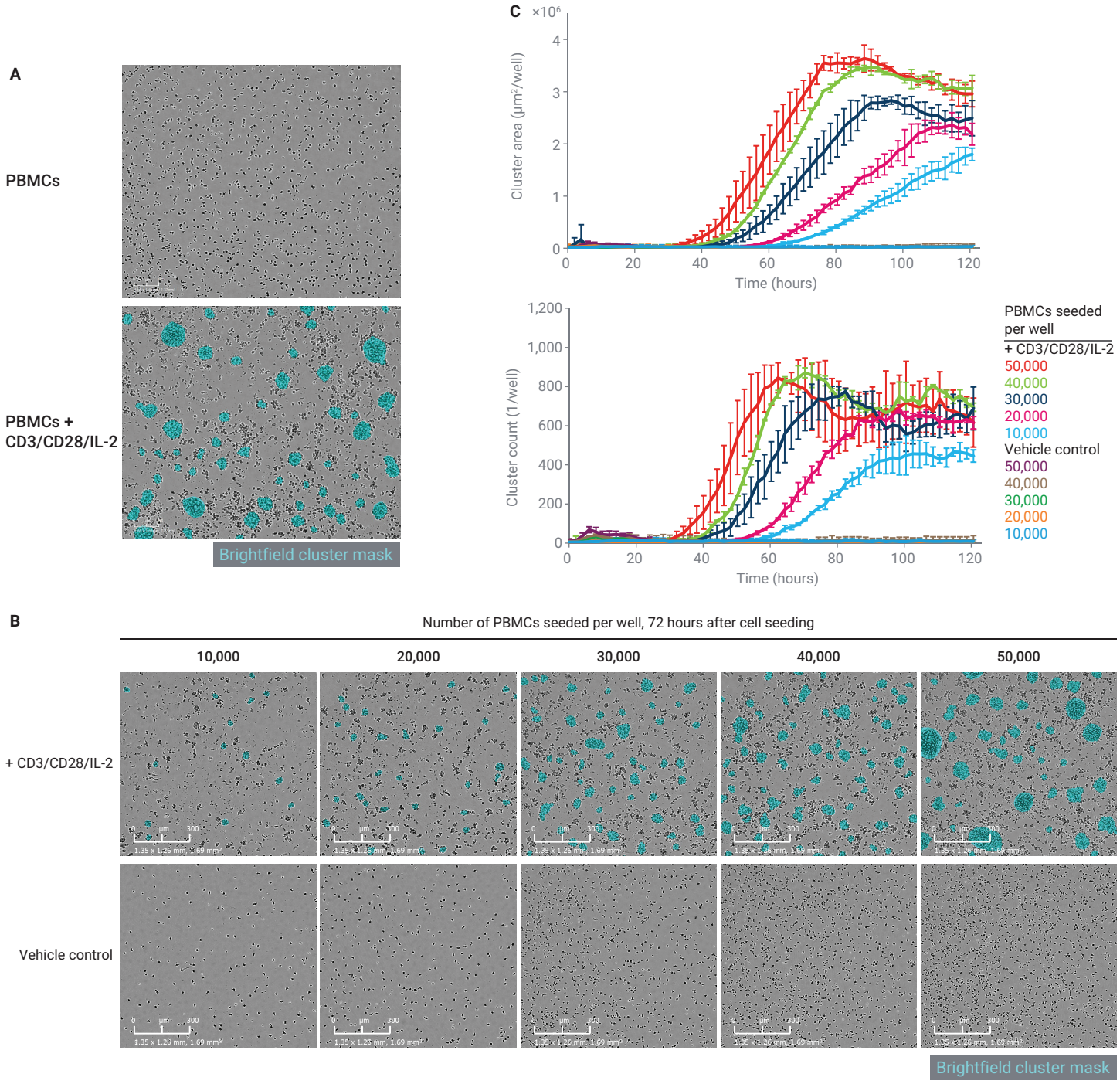

Figure 1. Monitoring *in vitro* T cell activation using the Immune Cell Clustering and Proliferation module on the Agilent xCELLigence RTCA eSight system. PBMCs were seeded on anti-CD3-coated cell culture plates, supplemented with anti-CD28 and IL-2. Clusters were recognized by xCELLigence RTCA eSight software automatically and masked in cyan. (A) Images at 72 hours after cell seeding with or without stimulation. (B) Images of PBMCs seeded at varying densities with or without stimulation. Images were collected by xCELLigence RTCA eSight every 4 hours; only representative images taken 72 hours after PBMC seeding are shown here. Scale bars = 300 µm. (C) Plots of cluster area and count as a function of time, respectively.

To study changes in cluster count and size at different seeding densities, PBMCs were serially diluted and seeded into 96-well plates. As shown in Figure 1B, small clusters merged into large ones (in a random fashion) over time. Cluster count and size increased with seeding density three days after CD3/CD28/IL-2 costimulation.

In Figure 1C, cluster count and size are plotted as a function of time and it can be seen that cluster formation begins 30 hours post seeding. Visually, cluster count and area gradually increased after 30 hours in correlation with initial seeding density. Importantly, the results shown in Figure 1C are consistent with the trends observed in Figure 1B.

In another experiment, activated T cells were labeled with an anti-CD45 antibody conjugated with BV421 and images were captured using the RTCA xCELLigence eSight system. Figure 2 shows cell clusters automatically recognized by xCELLigence RTCA eSight software (cyan mask) are consistent with those fluorescently labeled (blue clusters, pink mask outline), demonstrating the accuracy of the xCELLigence RTCA eSight label-free cluster recognition algorithm. One additional observation is that when overlaying Brightfield (cyan cluster mask) plus CD45 BV421 (pink mask outline), there are some subtle differences where very smaller clusters are recognized by fluorescent labeling, but not the Brightfield mask. If necessary, this can easily be adjusted using the area filter for further optimization.

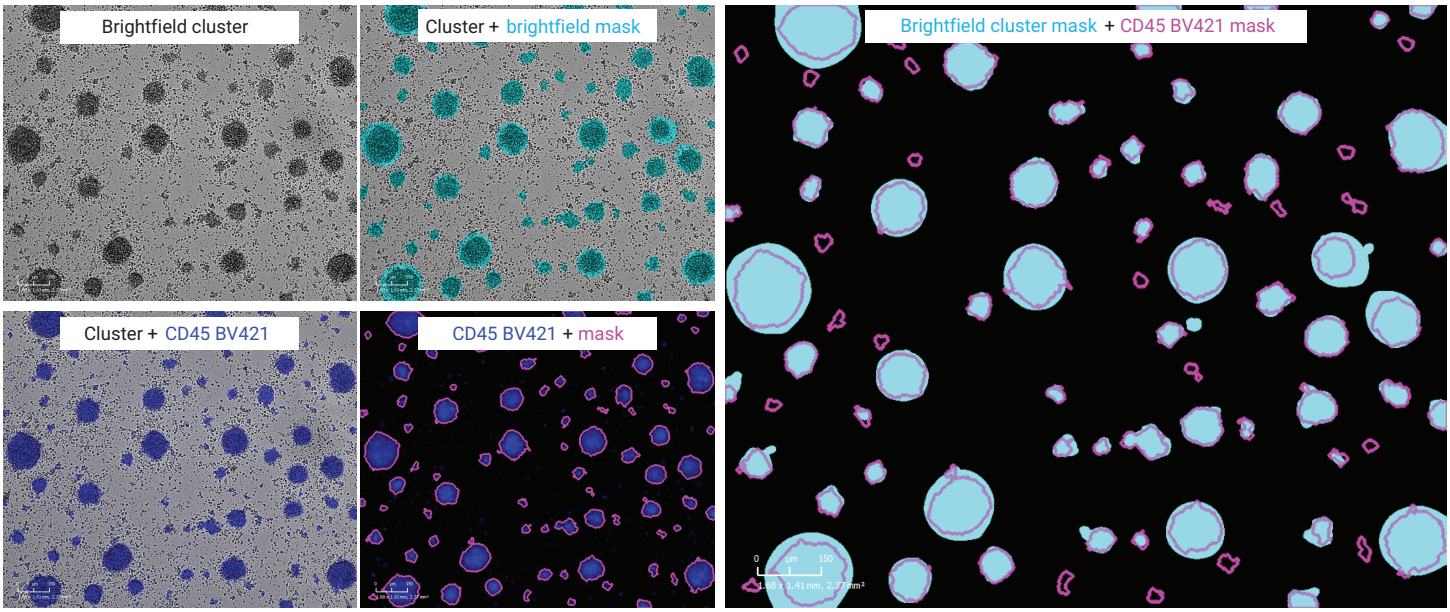

Figure 2. The cluster recognition based on brightfield by the Agilent xCELLigence RTCA eSight software (cyan mask) is consistent with the cluster recognition based on specific fluorescent labeling (pink mask outline). Pre-activated T cells were labeled by anti-CD45 BV421 antibody, and images were collected 16 hours later.

CAR-T cell proliferation in killing assays

Next, the killing of CD19-expressing Raji cells by CD19-targeting CAR-T cells was evaluated using the xCELLigence RTCA eSight system. K562 cells not expressing CD19 were used as a negative control. eLive Red–prelabeled anti-CD19 CAR-T cells were added to target cells and incubated overnight. Clusters that were characteristic of CAR-T activation formed after 24 hours, growing over time. Raji green cells that were co-incubated with CAR-T cells gradually reduced in number, while those without continued to proliferate (Figure 3).

Moreover, we compared xCELLigence RTCA eSight software cluster recognition (Figure 4A, cyan mask) with cluster recognition by the naked eye (Figure 4B, pink mask). Results showed that after 48 hours of co-incubation, the two are well matched, verifying the accuracy of the software in killing assays (Figure 4). Unsurprisingly, red fluorescent CAR-T cell aggregates were particularly bright at the cell cluster locations.

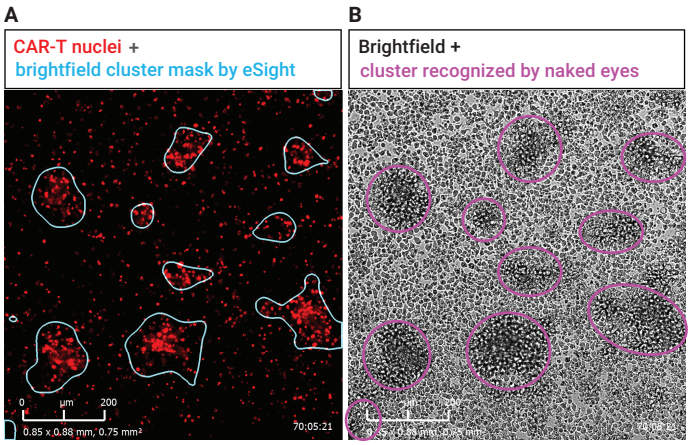

Figure 4. The brightfield-based cluster recognition by Agilent xCELLigence RTCA eSight software (A) is highly consistent with the cluster recognition by the naked eye (B). Representative images of CAR-T cell co-incubation with Raji cells after 48 hours are shown here.

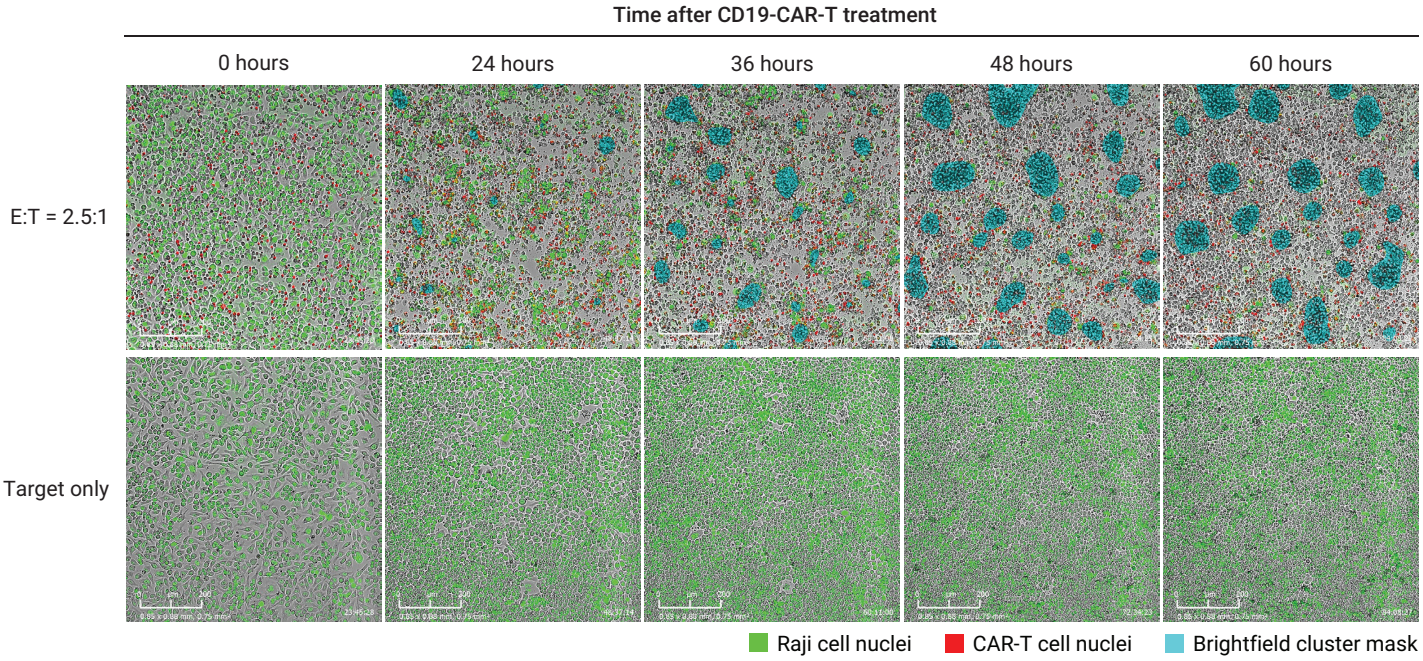

Figure 3. Select images demonstrate anti-CD19 CAR-T cell cluster formation and size increase over time when co-incubated with Raji cells. Raji cells were immobilized on the Agilent E-Plate VIEW microplate using anti-CD40 tethering reagent and allowed to proliferate overnight before CAR-T cells or medium control were added. Images were captured by the Agilent xCELLigence RTCA eSight instrument in real time, and cell clusters were recognized and masked in cyan. Representative images of E:T 2.5:1 at 0, 24, 36, 48, and 60 hours after co-incubation are shown. Due to certain challenges of the pulse labeling method (please see the previous application note "Optimizing Pulse Label Fluorescent Label Conditions and Image Acquisition Parameters" by Zhang *et al.*, 5994-5069EN)[7], eLive Red gets distributed into daughter cells and weakens as CAR-T cells proliferate.

Quantitative analysis of both imaging and impedance is shown in Figure 5. CAR-T activation and proliferation after antigen stimulation was quantified by cluster size obtained by xCELLigence RTCA eSight software. Changes in anti-CD19 CAR-T cell clusters when cocultured with Raji (Figure 5A) or K562 cells (Figure 5B) are plotted. Results demonstrate that CAR-T cells activate and cluster only after anti-CD19 CAR interacts with CD19 at the surface of Raji cells. Cluster area was positively correlated with time and the number of CAR-T cells seeded. At a 2.5:1 E:T ratio, CAR-T cells clustered about 20 hours after target cell seeding. In comparison, after coculture with K562, CAR-T cells were not activated, and clusters did not form without antigen stimulation (Figure 5B).

After activation and proliferation, the efficiency of CAR-T cells at killing Raji target cells was examined. Cellular impedance provides a sensitive readout of immobilized Raji cell count, independent of the fluorescent labeling. Decreasing cellular impedance over time is shown in Figure 5C, indicating that the killing effect of CAR-T cells on Raji cells depends on the number of CAR-T cells seeded (that is, higher E:T ratio, sharper decline). In contrast, CAR-T cells showed little to no killing of K562 cells, resulting in similar impedance plots with or without CAR-T treatment (Figure 5D).

Combining cellular impedance and imaging enables simultaneous monitoring of both CAR-T proliferation and potency without labels, in the same wells, and from varying perspectives. Imaging allows for clustering analysis—a direct way to evaluate CAR-T cell proliferation. However, since there are two types of cells in a single well, it is difficult to detect target cells solely through imaging. By nature, cellular impedance reflects the target cell status and viability, monitoring cell adherence and attachment strength to the E-Plate surface. Since dead cells detach from the surface, cytolysis can easily be measured as a decrease in Cell Index. Suspended CAR-T cells, meanwhile, contribute a negligible amount to the impedance signal. The xCELLigence RTCA eSight's dual readout provides rich information and sensitive, orthogonal results to reflect CAR-T cell potency more accurately than traditional assays, while reducing assay preparation time.

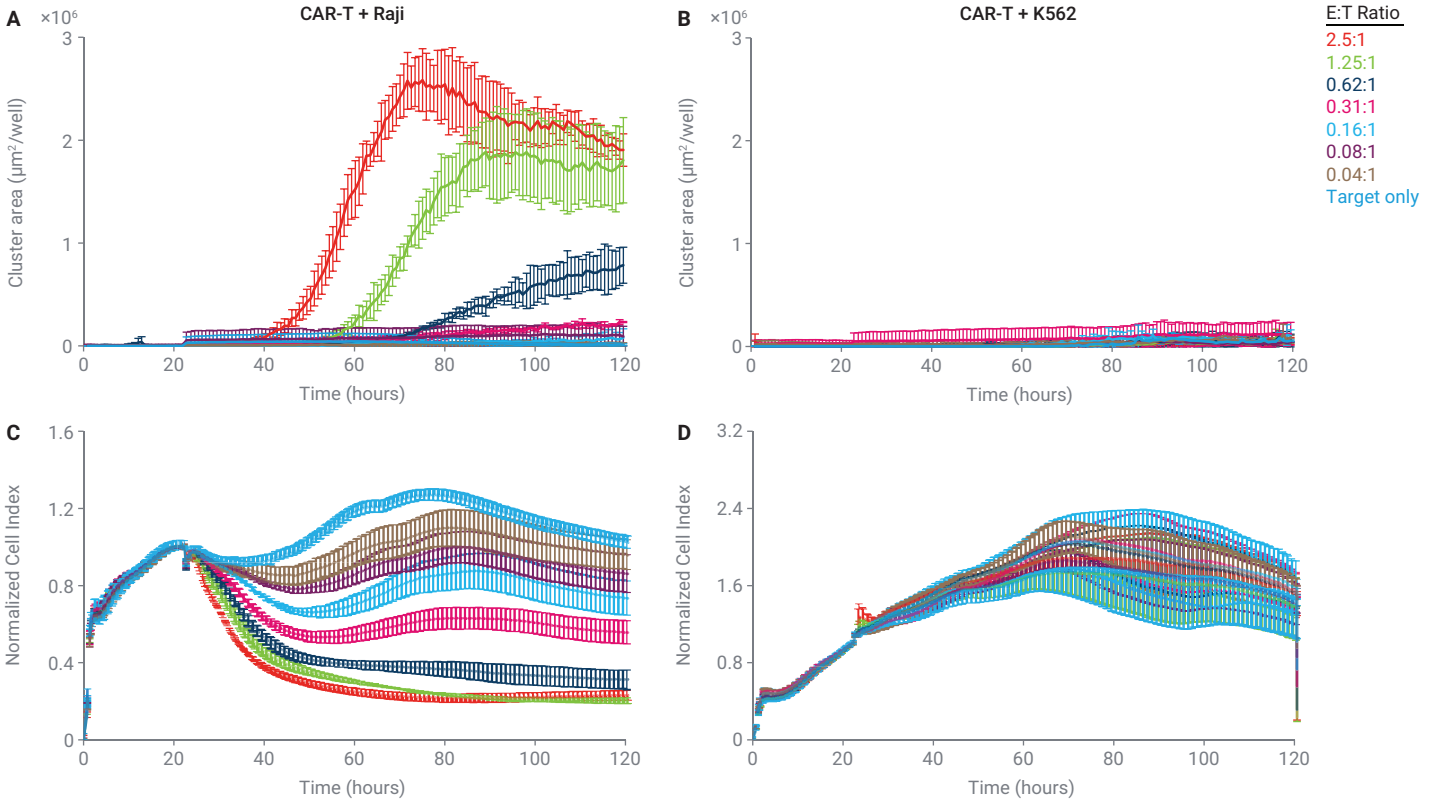

Figure 5. Changes in cell cluster size over time are highly correlated with cytolysis. (A) The plot of anti-CD19 CAR-T cell cluster area as a function of time when cocultured with Raji cells. (B) The plot of cluster area as a function of time when CAR-T cells were cocultured with K562 cells. (C) The plot of normalized Cell Index (impedance readout) over time when the CAR-T cells were cocultured with Raji cells. (D) The plot of normalized Cell Index (impedance readout) over time when the CAR-T cells were cocultured with K562 cells.

NK-92 cell proliferation in killing assay

Finally, we also evaluated the xCELLigence RTCA eSight's automatic recognition of NK-92 cluster formation during growth and cell killing. After allowing seeded A549 red cells to attach to the E-Plate and proliferate for 24 hours, NK-92 cells were added at E:T ratios of 6:1, 3:1, 1.5:1, 0.75:1, 0.38:1, 0.19:1, and 0, respectively. Unlike CAR-T cells (E:T 2.5:1), which formed clusters 24 hours after addition, NK-92 cells at an E:T of 6:1 quickly formed clusters as soon as they were added into the wells, and the clusters increased in size with time (Figure 6). A549 red cells co-incubated with NK-92 cells significantly decreased in population, in contrast to continued proliferation in their absence.

NK-92 activation and proliferation at different E:T ratios, as well as sequential killing of A549 red cells, were plotted using imaging and cellular-impedance-based readouts, respectively. The cluster area plot (Figure 7A) showed that NK-92 activation depended on the E:T ratio. At a 6:1 ratio, NK-92 cells caused the impedance signal to drop to zero, indicating that A549 cells were completely killed. Figure 7B shows that there is a stronger killing effect at higher E:T ratios.

In summary, NK-92 cell clustering highly correlates to killing efficacy. As with the CAR-T cell killing assay, the dual readout in the NK-92 killing assay provides rich information on both cell proliferation and target cell killing efficacy within the same wells. Differences in cluster formation kinetics or killing efficacy between two effector cell types can also be examined using the described assays.

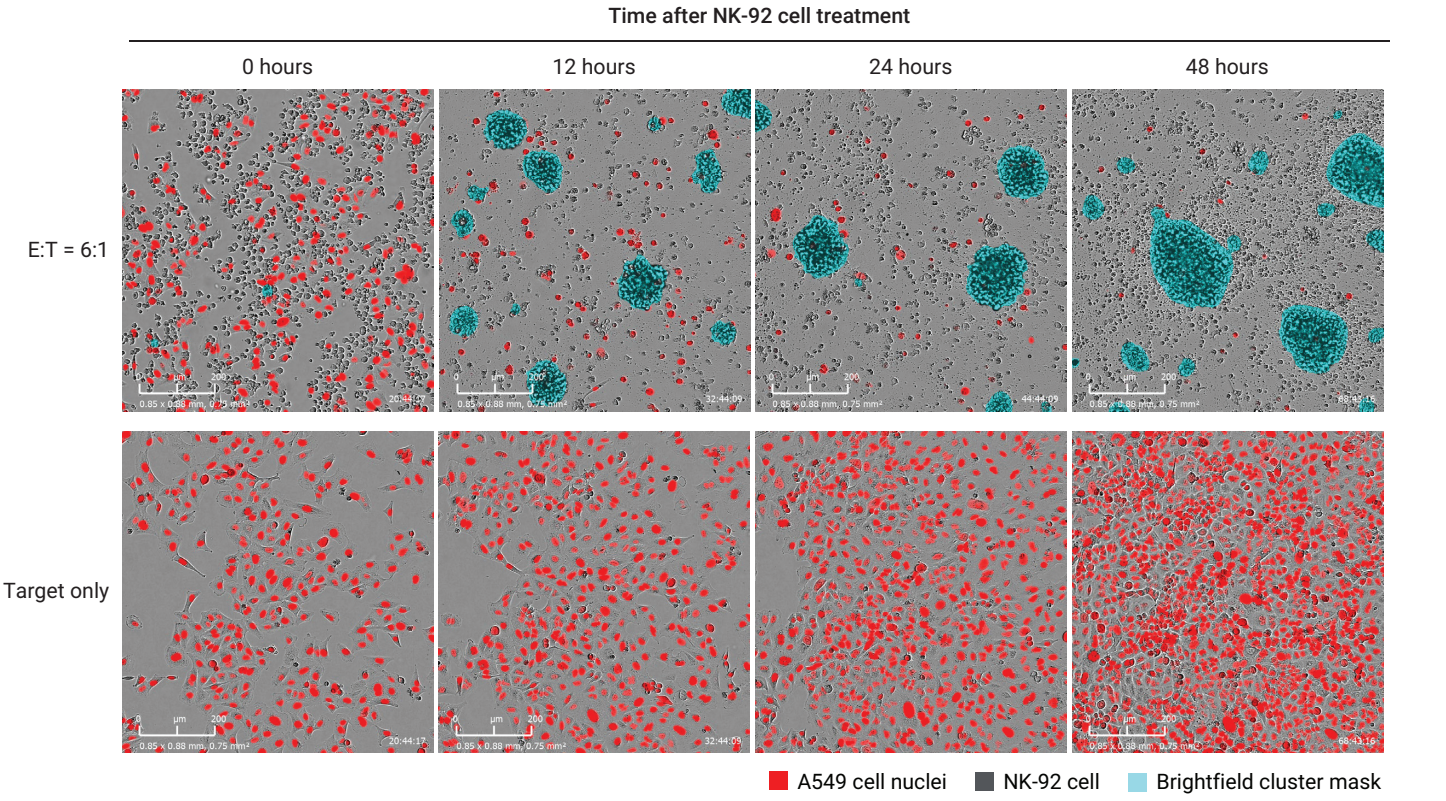

Figure 6. Selected images show the cluster recognition of NK-92 cells and cluster area increase over time. After treatment of A549 red cells with NK-92 cells at an E:T ratio of 6:1, the cluster area representing NK-92 activation was tracked. Representative images at 0, 12, 24, and 48 hours after NK-92 addition are shown.

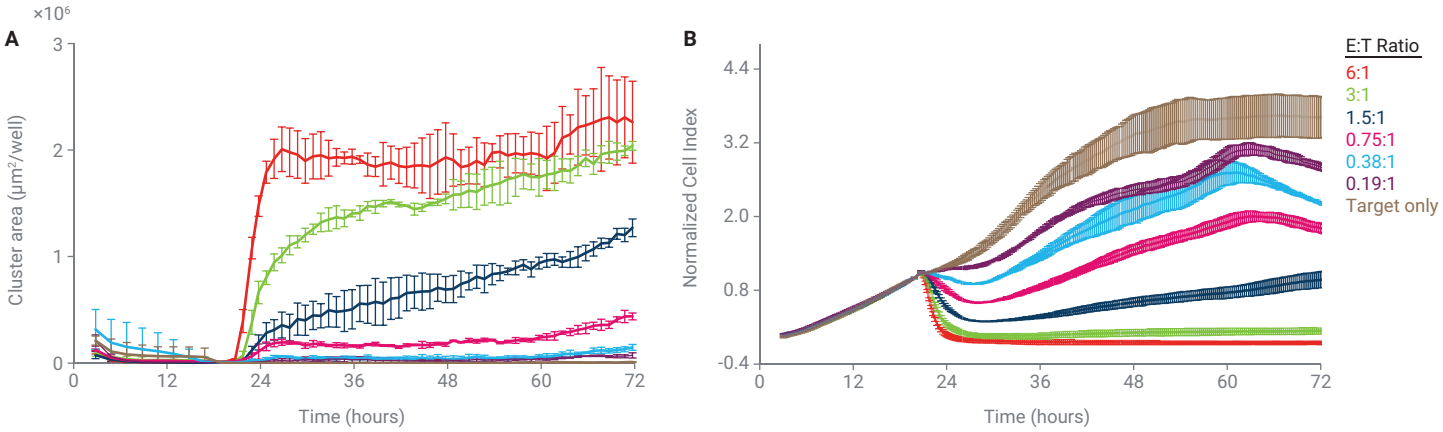

Figure 7. Correlating the killing effect of NK-92, detected in real time by impedance, with specific cellular activation revealed by live cell imaging. The cluster area and impedance signal were tracked after treating A549 red cells with varying numbers of NK-92 cells. (A) NK-92 cluster area as a function of time when A549 cells were treated with NK-92. (B) The normalized Cell Index as a function of time reflects NK-92 killing of A549.

Conclusion

The Immune Cell Clustering and Proliferation module on the Agilent xCELLigence RTCA eSight software automatically recognizes immune cell clusters (T cells, NK cells) from brightfield images without requiring additional fluorescent labeling. Cluster formation and any subsequent changes can be monitored in real time for several days within a climate-controlled incubator. The xCELLigence RTCA eSight software provides cluster size and count metrics, supporting quantitative analysis of immune cell activation and proliferation. When combined with cellular impedance, the killing efficacy of immune cells can be evaluated simultaneously. Overall, xCELLigence RTCA eSight provides a versatile method to assess and quantify various types of effector cells in real time. The multimodal data acquisition capabilities introduced by the xCELLigence RTCA eSight provide a simplified workflow to evaluate immune cell proliferation and cytotoxicity—an addition of immense value to the development of the immunotherapy field.

References

1. Zumwalde, N. A. *et al.* ICAM-1-Dependent Homotypic Aggregates Regulate CD8 T Cell Effector Function and Differentiation During T Cell Activation. *J. Immunol.* **2013**, *191(7)*, 3681–93.
2. Capitani, N.; Baldari, C. T. The Immunological Synapse: An Emerging Target for Immune Evasion by Bacterial Pathogens. *Front. Immunol.* **2022**, *13*, 943344.
3. Kim, M. *et al.* Multi-Cellular Natural Killer (NK) Cell Clusters Enhance NK Cell Activation Through Localizing IL-2 within the Cluster. *Sci. Rep*. **2017**, *7*, 40623.
4. Filippi, C. M. *et al.* Transforming Growth Factor-Beta Suppresses the Activation of CD8+ T-Cells when Naive But Promotes Their Survival and Function Once Antigen Experienced: a Two-Faced Impact on Autoimmunity. *Diabetes* **2008**, *57(10)*, 2684–92.
5. Farwell, M. D. *et al.* T Cells Modulate Glycans on CD43 and CD45 During Development and Activation, Signal Regulation, and Survival. *Ann. NY Acad. Sci*. **2012**, *1253*, 58–67.
6. Korell, F.; Berger, T. R.; Maus, M. V. Understanding CAR T Cell-Tumor Interactions: Paving the Way for Successful Clinical Outcomes. *Med. (NY)* **2022**, *3(8)*, 538–564.
7. Zhang, J. *et al.* Immune Cell Killing Assays Using xCELLigence RTCA eSight: Optimizing Fluorescent Labeling Conditions and Image Acquisition Parameters. *Agilent Technologies application note*, publication number 5994-5069EN, **2022**.

www.agilent.com/chem/esight

Printed in the USA, March 1, 2023
5994-5767EN

Agilent
Trusted Answers